Monomer Exchange Dynamics of Self-Assembled Surfactant Monolayers at the Solid–Liquid Interface

Simon Schrödle and Geraldine L. Richmond*[a]

Self-assembly of surface-active agents at solid–liquid interfaces is critical for many processes in nature and technology, including the stability of suspension, detergency, wetting and mineral separation.[1] Historically, a detailed understanding of nanometer-scale layers has emerged. However, surprisingly little is known about their dynamics—the key to non-equilibrium phenomena.[2] Even in equilibrium, there is constant exchange of monomers between bulk and monolayer. Determination of the associated rate constants has been undertaken by evaluating adsorption and desorption kinetics.[3] These methods are not practical near equilibrium adsorption as they rely upon a changing surface concentration. Hence, little can be learned about the true equilibrium state of a monolayer. The importance of dynamical properties at solution interfaces has long been realized and relaxation techniques, utilizing the system's response to perturbation from equilibrium, have developed into powerful tools.[2] Unfortunately, these methods do not adapt easily to the rather slow kinetics typically found at the solid–liquid interface.

The nature of the solid–liquid boundary as a buried interface, together with the vanishingly small fraction of monolayer to bulk molecules poses a serious experimental challenge. Certain spectroscopic techniques are applicable, and in fact infrared attenuated reflection spectroscopy (IR-ATR) has been used[4,5] to study exchange reactions of aggregates at interfaces. However, this linear IR technique probes an interfacial region extending to hundreds of nanometers—including molecules far beyond the monolayer. Higher interfacial specificity is obtained with nonlinear optical methods.[6,7] Kinetic studies at the air–water interface by second harmonic generation have been reported.[8,9] The related but more powerful vibrational sum-frequency spectroscopy (VSFS) exploits resonant effects of vibrational transitions,[6,7] and has demonstrated its applicability for the study of monolayers at mineral–water interfaces.[10,11] However, its current use for such systems has heretofore been limited to static investigations. Herein, we exploit a wide-band, rapidly tunable IR source within a VSFS system to investigate dynamic phenomena.[12]

[a] Dr. S. Schrödle, Prof. Dr. G. L. Richmond
    Department of Chemistry, University of Oregon
    1253 University of Oregon, Eugene, Oregon 97403 (USA)
    Fax: (+1) 541-346-5859
    E-mail: richmond@uoregon.edu
    Supporting information for this article is available on the WWW under
   http://www.chemphyschem.org or from the author.

A simplified, three step, monomer exchange process is described in Figure 1. The surfactant (sodium dodecanoate, C12) is first released from the monolayer (rate constant k_D). Secondly monomer adsorption occurs from the bulk into a randomly oriented state (k_A) on the substrate (fluorite CaF_2). Finally an ordered monolayer is reformed (k_O).
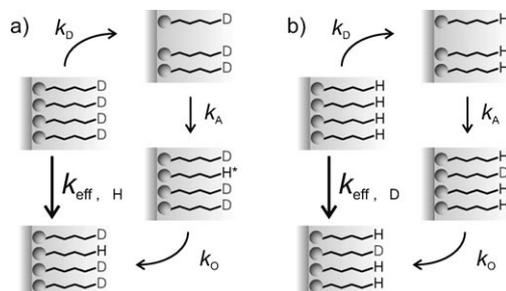
Figure 1. Idealized monomer exchange mechanism. Isotope labeling of C12 is indicated by H (CH_3 terminus) or D (CD_3 terminus). Exchange reaction starting from a a) fully deuterated or b) hydrogenated monolayer.

During the experiment, exchange kinetics, characterized by $k_{eff,H}$ or $k_{eff,D}$, were followed by measuring the resonance response of the second-order nonlinear susceptibility $\chi^{(2)}$ at frequencies characteristic of the carboxylate headgroup (νCO, 1453 cm^{-1}) as well as the symmetric stretch of the surfactant's terminal CH_3 group (νCH_3, 2873 cm^{-1}). Unlike linear spectroscopies, VSFS utilizes a coherent process within the temporal and spatial overlap of a visible (VIS, 532 nm) and IR beam (tunable).[6,10] In our experiment, the intensity of the sum-frequency (SF) signal is directly proportional to the square of the interface susceptibility, $\chi^{(2)}_{yyz}$, which is a measure for the number of oriented molecules at the interface (see Supporting Information).[6] Note that this intrinsic sensitivity for molecular orientation has important consequences for the effective (observable) exchange rates (Figure 1): $k_{eff,H}$ encompasses all three steps with only the final species being SF-active, whereas $k_{eff,D}$ is determined by the desorption process (k_D), as this key step reduces the number of SF oscillators.
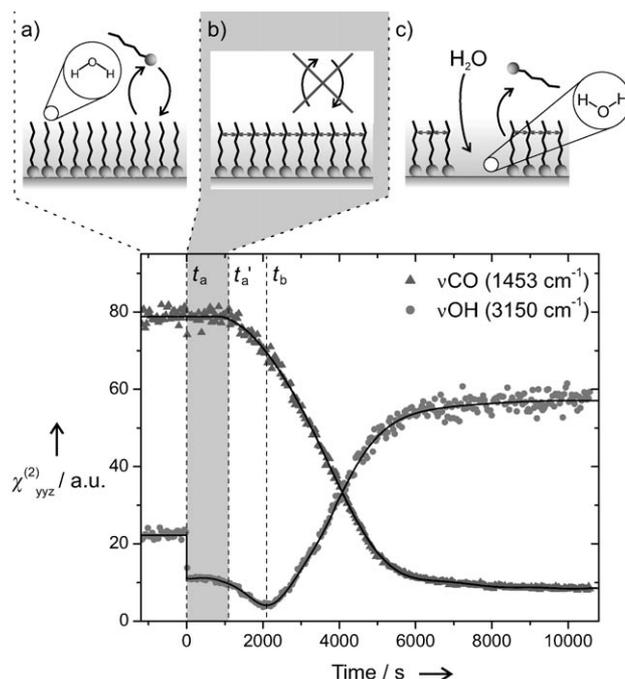
Typical experimental data is presented in Figure 2. The total adsorption density measured by the νCO susceptibility ($\chi^{(2)}_{1453,norm}$, Figure 2 a), remains constant as expected from the similarity of C12–H and C12–D. This demonstrates equilibrium adsorption. From the νCH_3 response, the mole fraction of hydrogenated surfactant in the monolayer, f_{2873}, was derived (see Supporting Information). Two types of experiments were performed: one starting from a fully deuterated monolayer (Figure 2b), the other starting from a hydrogenated monolayer (Figure 2c). In both cases, the rapid onset of the exchange reaction after exposing the monolayer to a bulk solution with opposite surfactant isotopic labeling suggests a fast exchange of surfactant monomers in the region adjacent to the monolayer. Surfactant molecules close to the interface but not incorporated into the monolayer are replaced on a timescale much faster than the observed kinetics, in agreement with other
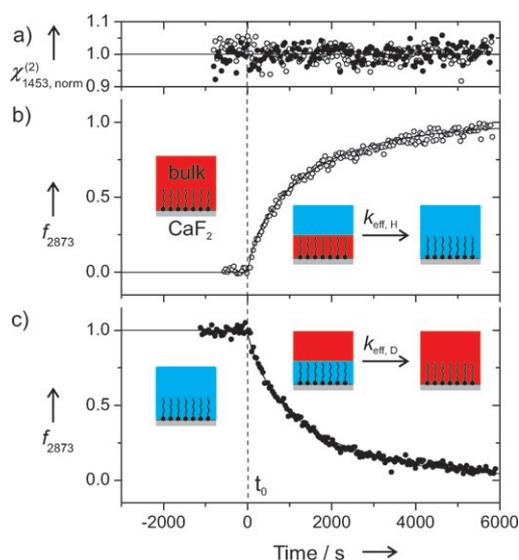
Figure 2. Monomer exchange kinetics of sodium dodecanoate at the fluorite–water interface (○: fully deuterated, ●: fully hydrogenated monolayer for $t < t_0$). a) Normalized nonlinear optical response of the carboxylate head-group, $\chi^{(2)}_{1453,\ norm}$. b) Exchange kinetics ($k_{eff,H}$) of a deuterated monolayer, and c) of a hydrogenated monolayer ($k_{eff,D}$). At t_0, the bulk liquid phase was replaced by a surfactant solution of equal concentration (10 μM) but opposite isotope labeling. In the pictorial representations, blue areas correspond to hydrogenated, red areas to deuterated surfactant molecules.

Figure 3. Desorption kinetics of an equilibrated C12–H monolayer. At time t_a, the surfactant solution was replaced by neat water. Surface coverage is followed by the νCO response at 1453 cm^{-1} (▲) and remains virtually constant until t_a'. At t_b, the phase of the νOH resonance (●) shifts by π, indicating a flip of the interfacial water molecules due to surface charge reversal. Also given is a schematic view of the monolayer a) in equilibrium with a bulk surfactant solution, b) during the induction period (grey area; arrows indicate a non-equilibrium state of the monolayer), and c) during desorption. The predominant orientation of water molecules above the monolayer and at the CaF$_2$ surface is also shown.

studies of bulk micelles or loosely bound surfactant aggregates, which are characterized by typical exchange rates of $\sim 10^4$ s^{-1} and ~ 1 s^{-1}, respectively.[4] The bulk concentrations (10 and 30 μM) used for this study are both above the hemi-micellar critical limit (~ 1 μM, see Supporting Information), but well below the critical micellar concentration (~ 24 mM).[13] Therefore, surfactant molecules are all monomeric in the bulk. If the observed exchange reactions were induced by collisions between bulk molecules and monolayer, exchange rates would be strongly correlated with bulk concentration. Kinetic analysis however revealed no significant effect of bulk concentration on the exchange rate constants $k_{eff,H}$ and $k_{eff,D}$, which relate to the exchange reaction between a monolayer, initially composed of neat C12–D (Figure 2b) or C12–H (Figure 2c), and a liquid phase containing C12–H or C12–D, respectively. Both constants were found to be equal at an average value of $k_{eff} = (8.1 \pm 2.0) \times 10^{-4}$ s^{-1}. The desorption reaction (k_D, Figure 1) is then rate-determining and the ordering step (k_O) is very fast. The fraction of disordered (i.e. non SF-active) molecules in the equilibrium monolayer must therefore be small.

For comparison, non-equilibrium desorption experiments (similar to those reported by others and used to characterize exchange dynamics[3]) were performed (Figure 3). These experiments comprise flushing of a fully established, equilibrium monolayer (Figure 3a) with neat water (for $t > t_a$), while the SF-responses at 1453 and 3150 cm^{-1} are continuously monitored. From the temporal profile of the surface density of SF-active carboxylate (νCO, 1453 cm^{-1}), monomer desorption into neat water is obviously much slower initially than expected from the equilibrium exchange rate and characterized by a substan-

tial induction period (Figure 3b, $t_a < t < t_a'$). As part of the desorption experiments, the number of oriented water molecules in the interfacial region was concurrently measured via their SF intensity at 3150 cm^{-1} (νOH). The phase of the νOH response obtained from spectral fits[10] demonstrates that water molecules above an intact monolayer are oriented with their oxygen atoms pointing toward the bulk liquid phase. Accordingly, the monolayer is negatively charged at full coverage, a phenomenon commonly referred to as overcharging.[10] When flushing of the monolayer with neat water starts at t_a, the intensity associated with interfacial water molecules immediately drops by 50% (Figure 3). This indicates a considerably diminished number of highly ordered (symmetrically coordinated) water molecules in the layer immediately above the monolayer. These changes occur despite virtually constant monolayer coverage during the induction period (Figure 3b, $t_a < t < t_a'$) and are, as can be shown by similar experiments in the presence of background electrolyte, not caused by the change in bulk ionic strength at t_a. Other factors besides simple electrostatic effects seem to be responsible for the significant difference of the hydrogen-bond structure near an equilibrium or non-equilibrium monolayer, respectively. After the induction period, monomer desorption slowly ensues. The phase of the VSFS resonance and thus the predominant orientation of interfacial water molecules remain unchanged until, very gradually,

the point of charge neutrality is reached at t_b (minimum of the νOH response[10]). At this time a degree of structure returns to interfacial water, which is, with the breakdown of the monolayer, at least partly exposed to the uncovered fluorite surface bearing positive charge. At t_b, the phase of the VSFS response at 3150 cm^{-1} shifts by π, because interfacial water molecules have now flipped to an orientation with their hydrogen atoms pointing toward the liquid phase. With continued release of monomers, the defect concentration of the monolayer reaches a critical level and desorption then proceeds at a rapidly increasing rate, for example, along boundaries of water-rich surface regions and remaining monolayer domains. While a detailed kinetic analysis of the desorption process will be presented elsewhere, we derived desorption rates from a numerical analysis of the νCO data of Figure 3. It was found that the desorption rate increases by several orders of magnitude after the start of flushing with neat water, from nearly zero at t_a to $\sim 1\times10^{-3}$ s^{-1} at low coverage (Figure 3, $t > 4000$ s), which is similar to k_{eff}, the rate of equilibrium monomer exchange.

In conclusion, the nonlinear spectroscopic approach presented here reveals the dynamism of self-assembled monolayer interfaces. The results also demonstrate the importance of understanding the structure of liquid adjacent to the monolayer as this structure governs energetic barriers and thus system dynamics. From this realization we may also infer a reason for the wide variation in reported rates of equilibrium and non-equilibrium kinetic parameters:[3,4,14] Only very few molecules can be withdrawn from the monolayer at a given time and if they are not replenished instantly, further desorption incurs high energetic cost because it disturbs the highly coordinated hydrogen-bond structure of water molecules within the interfacial region. Finally, at low monolayer coverage, desorption rates approach values similar to the monomer exchange rate under equilibrium conditions, because the energetic advantage inherent to an intact monolayer vanishes.

Experimental Section

All experiments were performed using an EKSPLA PL2143 A/SH Nd:YAG laser producing 1064 and 532 nm radiation (30 ps pulse duration, 10 Hz repetition rate). A tunable IR beam was generated by an EKSPLA PG501/DFG2-10P optical parametrical oscillator/amplifier with an AgGaS$_2$ difference frequency stage (2.3 to 10 μm). For the current VSFS experiments, the IR and visible (532 nm) laser beams were incident on a CaF$_2$ prism (68°/68°), aligned to near critical angle at the interface, 17° and 20.5°, respectively. High-efficiency filters and dispersive optics were used to select the sum-frequency photons which were metered by a photomultiplier. Beam generation, spatial overlap and data acquisition were controlled by a computer and LabView Software. A peristaltic pump was used to constantly flush the prism surface with fresh sample liquid. Materials in contact with the sample were PTFE and PCTFE (Kel-F). Further details of the experimental procedures and data analysis are provided in the supporting information.

[1] D. Myers, *Surfaces, Interfaces, and Colloids: Principles and Applications*, 2nd ed., John Wiley & Sons, New York, **1999**.
[2] S. S. Dukhin, G. Kretschmar, R. Miller, *Dynamics of Adsorption at Liquid Interfaces*, Elsevier, Amsterdam, **1995**.
[3] M. L. Free, J. D. Miller, *Langmuir* **1997**, *13*, 4377–4382.
[4] S. C. Clark, W. A. Ducker, *J. Phys. Chem. B* **2003**, *107*, 9011–9021.
[5] A. Khan, W. A. Ducker, M. Mao, *J. Phys. Chem. B* **2006**, *110*, 23365–23372.
[6] G. L. Richmond, *Chem. Rev.* **2002**, *102*, 2693–2724.
[7] M. Buck, M. Himmelhaus, *J. Vac. Sci. Technol. A* **2001**, *19*, 2717–2736.
[8] T. Rasing, T. Stehlin, Y. R. Shen, M. W. Kim, P. Valint, Jr., *J. Chem. Phys.* **1988**, *89*, 3386–3387.
[9] A. Castro, S. Ong, K. B. Eisenthal, *Chem. Phys. Lett.* **1989**, *163*, 412–416.
[10] K. A. Becraft, G. L. Richmond, *J. Phys. Chem. B.* **2005**, *109*, 5108–5117.
[11] K. A. Becraft, F. G. Moore, G. L. Richmond, *J. Phys. Chem. B* **2003**, *107*, 3675–3678.
[12] J. Liu, J. C. Conboy, *J. Am. Chem. Soc.* **2004**, *126*, 8376–8377; T. C. Anglin, J. Liu, J. C. Conboy, *Biophys. J.* **2007**, *92*, L01 L03.
[13] P. Mukerjee, K. J. Mysels, K. *Nat. Stand. Ref. Data Ser.* **1971**, *36*, 137.
[14] E. S. Pagac, D. C. Prieve, R. D. Tilton, *Langmuir* **1998**, *14*, 2333–2342; F. Tiberg, B. Jönsson, B. Lindman, *Langmuir* **1994**, *10*, 3714–3722.